Lars Heinke and Christof Wöll

SURFACE-MOUNTED METAL-ORGANIC FRAMEWORKS: CRYSTALLINE MATRICES FOR STUDYING MOLECULAR INTERACTIONS

Metal-Organic Frameworks are crystalline coordination poly-mers, which represent a new, interesting class of porous sol-ids. They are fairly stable, exhibit well-defined mechanical prop-erties, and can be prepared in a highly reproducible fashion on solid substrates. We demonstrate here that these crystal-line, highly ordered porous coatings are well suited as model systems to study molecular interactions in porous media in a quantitative fashion, including diffusion and optical switching between different molecular states. In addition, they are also qualified to study electrical transport through molecular frame-works and transfer of optical excitations. Because of their crys-talline nature, they are well-suited for quantitative compari-sons with results from theoretical work.

INTRODUCTION

Metal-Organic Frameworks, MOFs, are a new class of crystalline, highly porous molecular frameworks, which offer a huge poten-tial, not only for various technical applications in the field of gas storage and separation but also as a model system for funda-mental studies on molecular interactions. The introduction of this new type of crystalline coordination networks (CCNs) creat-ed a considerable excitement and a huge rush for the discovery of new types of these compounds.[1] Today, about 20 years after their introduction, more than 70.000 structurally characterized examples of this class have been reported.[2] Since MOFs are assembled by combining different types of molecular building blocks, namely di- or higher topic organic linkers and metal or metal-oxo nodes, the maximum number of these compounds is virtually unlimited.

Some of the fascinating properties of MOFs result from the fact that this class of materials is not only crystalline but also po-rous. The largest pore size reported so far has a diameter of around 10 nm.[3] Since basically each organic molecule can be modified by addition of opposite carboxylic acid groups or pyridine units to become a potential ditopic linker, the num-ber of possible MOF structures by far exceeds the number

of already known structures.[2] Recent papers have reported simulations for more than a million of these compounds.[4] This huge chemical space spanned by this type of materials not only offers an enormous potential for material science, it also is very attractive with regard to providing well-defined matrices for carrying out reference experiments to determine fundamental physico-chemical properties. The availability of a well-defined, crystalline porous matrix into which guest mole-cules can be loaded allows for a number of systematic spectro-scopic investigations. In contrast to solvents, MOFs provide a strictly periodic, structurally very well-defined environment. The environment is strictly identical for each embedded guest mol-ecule. In this respect, MOFs also outperform noble-gas guest matrices,[5] where the environment surrounding the embedded guest is certainly non- or weakly-interacting, but the inherent structural inhomogeneity of the local environment always re-sults in inhomogeneous broadening of the embedded guest's spectroscopic features, such as vibrational bands.

In this short overview we will discuss a number of examples where MOFs and in particular SURMOFs (Surface-Mounted Metal-Organic Frameworks) are used to provide well-defined environments to precisely determine quantities of importance for physical chemistry, in particular activation energies for the *cis*-to-*trans* isomerization of a prototype photoswitchable mole-cule, azobenzene, for diffusion experiments, and for transport of electrical charges.

We will also discuss the specific advantages of SURMOFs, thin, crystalline and highly ordered MOF films which are grown using a layer-by-layer (lbl) method, see Figure 1. This approach dif-fers from the conventional solvothermal method do synthesize MOF powders[1] in that the reactands are not mixed and then heated, but kept separately. Assembly of well-defined, highly oriented MOF thin films on appropriately functionalized sub-strates is achieved by subsequent immersion in different solu-tions containing the metal source and the organic ligands. This liquid-phase (quasi-) epitaxy (LPE) not only allows for the fabri-cation of well-defined electrical contacts to MOF-based materi-

Dr. Lars Heinke
Karlsruher Institut für Technologie (KIT)
Institut für Funktionelle Grenzflächen (IFG)
Hermann-von-Helmholtz-Platz 1, D-76344 Eggenstein-Leopoldshafen
Tel.: +49-721-608-22319
E-Mail: lars.heinke@kit.edu

Prof. Dr. Christof Wöll
Karlsruher Institut für Technologie (KIT)
Institut für Funktionelle Grenzflächen (IFG)
Hermann-von-Helmholtz-Platz 1, D-76344 Eggenstein-Leopoldshafen
Tel.: +49-721-608-23934
E-Mail: christof.woell@kit.edu
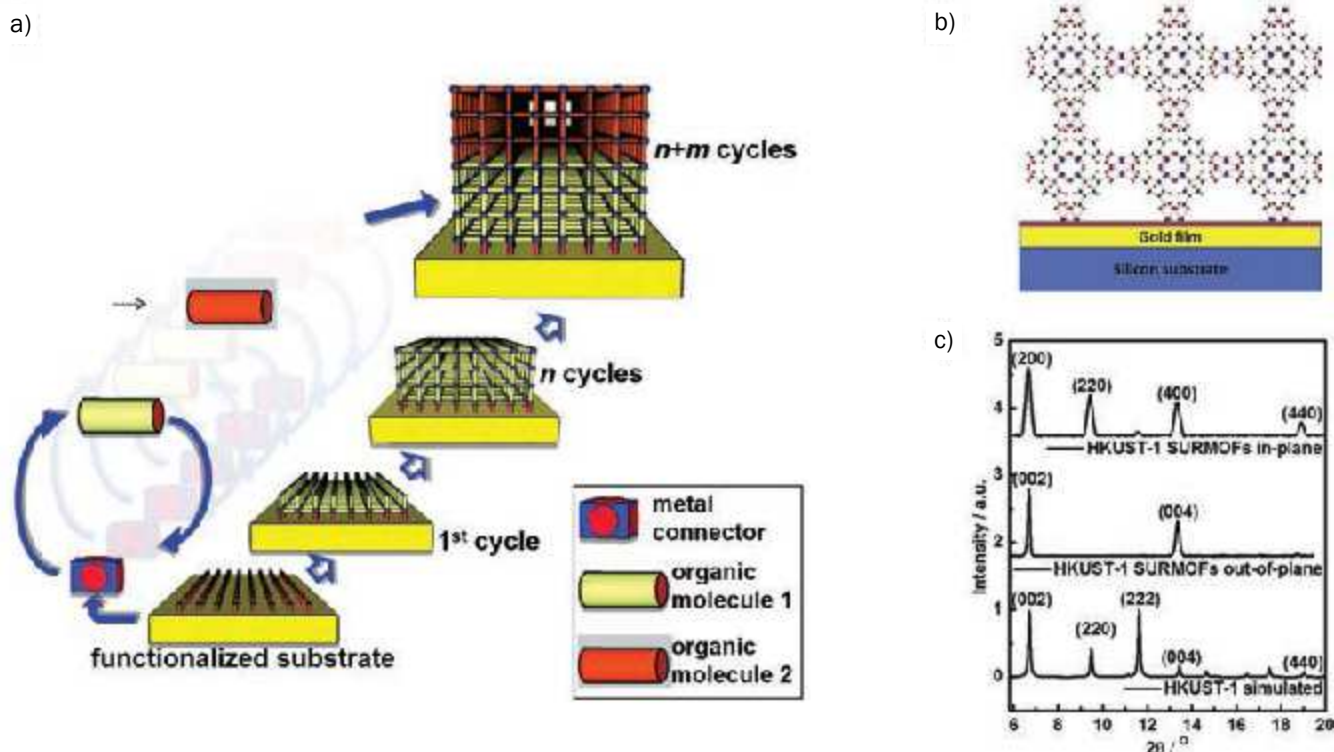
Fig. 1: Sketch of the SURMOF synthesis. a) The MOF films are prepared in a step-by-step fashion by alternatively exposing the functionalized substrate surfaces to the solutions of the metal nodes and of the organic linker molecules. By exchanging the organic linker molecules and/or the metal nodes during the synthesis, SURMOFs with different structures can be grown on top, resulting in multi-layered structures. b) Sketch of HKUST-1 SURMOF grown in (100) orientation on gold-coated silicon. c) In-plane and out-of-plane X-ray diffractograms recorded for HKUST-1 SURMOFs compared with the calculated diffractogram. Reproduced with permission form ref. [9]

als, but also for the fabrication of hetero-multilayers. In particular, the hetero-interfaces within such structurally well-defined multilayers allow for fundamental studies on the transfer of optical excitations and charge carriers across organic-organic interfaces.[6] For more details on the lbl synthesis of SURMOFs the reader is referred to recent literature.[7, 8]

MOF MECHANICAL PROPERTIES

As a result of their well-defined, crystalline structure, many of the physical properties of MOFs can be predicted in a straight-forward fashion. In previous work, for high quality SURMOFs, Young's modulus could be determined by applying standard indentation techniques. The value determined in these experiments, 9.3 GPa, is substantially higher than for conventional organic polymers and is in very good agreement with the results of theoretical work obtained using force-field calculations (10 GPa for HKUST-1, ref.[10])

MOF materials are also interesting because they exhibit a negative thermal expansion coefficient. By *in-situ* heating out-of-plane and in-plane X-ray diffractometry for SURMOFs mounted on Si substrates (which exhibit a positive thermal expansion), the resulting anisotropic expansion revealed an expansion [$\alpha_{SURMOF,in-plane} = (11.7 \pm 3.7) \times 10^{-6}$ K^{-1}] parallel to the substrate and a large contraction [$\alpha_{SURMOF,out-of-plane} = (-75 \pm 16) \times 10^{-6}$ K^{-1}] in *z* direction, i.e. perpendicular to the surface.[9] The analysis of this anisotropic thermal expansion behavior allows for the direct determination of another important elastic constant, the

Poisson's ratio, yielding a value of 0.69 ± 0.37 for HKUST-1 MOFs. It is remarkable, that HKUST-1 SURMOFs demonstrated a pronounced stability under heating/cooling cycles, though there is a pronounced mismatch of thermal expansion coefficients of the thin film and the substrate. This demonstrates that such coatings are well suited for integration into thermal-response devices. It should be noted, that the experimentally determined values for the elastic constants agree very well with computational results, which can be carried out in a straight-forward fashion for these crystalline, well-defined materials.

MOF THIN FILMS WITH VERY LOW DEFECT DENSITY

A high structural quality combined with a low density of defects is desirable for many applications of MOF thin films, for instance as sensor or optical devices. In several cases it has been demonstrated that the structural quality of SURMOFs is substantially higher than that of powder materials obtained by conventional solvothermal synthesis. Such powders are also not well suited for optical applications and for a thorough characterization of MOF absorption properties, since the scattering of light by the nm- to mm-sized powder particles can be considerable. Since SURMOFs with thicknesses below 100 nm typically show no charging effects when exposed to X-ray light, XPS (x-ray photoelectron spectroscopy) measurements can be carried out in a straightforward fashion.

In the case of MOFs containing under-coordinated metal sites, IR-studies of small molecules adsorbed at such sites
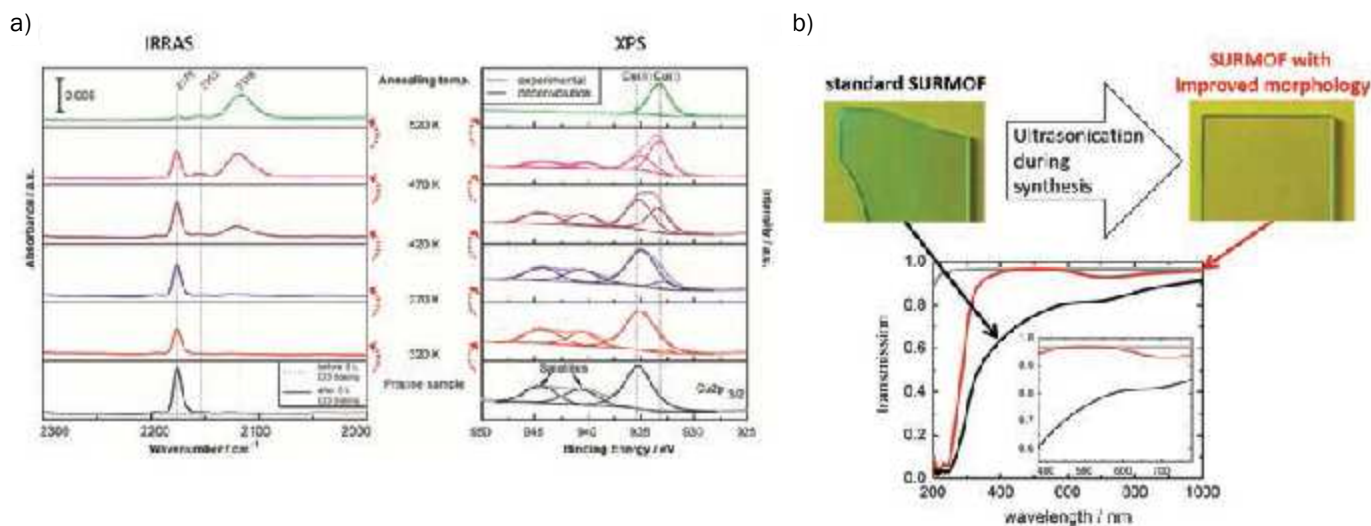
Fig. 2: SURMOF quality. a) UHV-IRRA spectra (left) and XPS curves (right) of a UHM-3 SURMOF sample in a pristine state, and after successive annealing at 320 K, 370 K, 420 K, 470 K, and 520 K. At first and after each annealing, the sample was cooled down to 110 K before the measurements were carried out. XPS data for the copper $2p_{3/2}$ region are shown. XPS experimental curves are depicted with circles and the deconvoluted curves according to the Cu(I) and the Cu(II) populations with plain lines. IRRAS spectra were acquired before (dashed line) and after (plain line) a 5 Langmuir CO dosing. Reproduced with permission form ref. [12] **b)** Cleaning the surface of the MOF thin films during the synthesis by ultrasonication results in an improved transparency, which can be seen by the naked eye. While the standard HKUST-1 SURMOF has the typical turquoise color, high-quality HKUST-1 SURMOFs prepared with ultrasonication are almost transparent. UV-vis transmission spectra show that the high-quality SURMOF (red spectra) has a tremendously higher transparency than the standard SURMOF (black spectra), especially in the visible range, which is shown in the inset. The transmission spectrum of the quartz glass substrate is the grey line. Reproduced with permission form ref. [13]

can be used to characterize defects. In case of HKUST-1, CO molecules bound to Cu^{++} ions exhibit IR-bands of 2179 cm^{-1}, whereas Cu$^+$-species cause a shift by approximately 60 cm^{-1} to 2121 cm^{-1}.[11] A combination of XPS and IRRAS allowed to demonstrate that HKUST-1 SURMOFs prepared by the layer-by-layer process exhibit defect densities lower than normal bulk samples, with a density of the most common defect, missing linkers, as low as 3-4 %.[11]

Interestingly, in a different type of MOFs, UHM-3 which is also formed from Cu^{++} dimers, the defect density was found to be much lower. The XPS results revealed a Cu$^+$ concentration of below 1 %. The defect concentration in these SURMOFs could be strongly increased by heating the samples, Figure 2a. The concentration of Cu$^+$ could also be monitored by recording IR-spectra of the CO molecules adsorbed at the Cu ions.[12]

In a later work, it was found that the quality of the SURMOF thin films can be significantly improved by optimizing the conditions of the lbl synthesis. By using a dipping robot combined with an ultrasonic bath for a more thorough rinsing of the sample surface during the synthesis, the surface roughness could be strongly reduced. At the same time the morphology was found to become substantially more homogeneous, as demonstrated by atomic force microscopy and scanning electron microscopy[13]. In addition, as clearly visible to the naked eye and also shown by means of UV-vis spectroscopy (see figure 2b), the optical transparency is remarkably improved by employing the ultrasonic treatment during synthesis. While the samples prepared using the regular lbl-process appear opaque and turquoise, the samples prepared using the same reactants but with ultrasonication are optically clear and show no surface scattering of light. These high-quality SURMOF films are therefore suitable for various optical applications and in particular for a thorough characterization of MOF

optical properties. For example, the higher optical film quality enabled the experimental determination of the band gap in HKUST-1 by means of ellipsometry.[14] Such investigations are difficult for MOF powders since scattering effects hinder the recording of high-quality UV-Vis spectra.

DETERMINING ELECTRICAL CONDUCTIVITY

Despite the fact that MOFs were originally developed for applications in gas storage and separation[15], in recent years applications of these highly flexible materials as active and passive components in electronic devices have attracted considerable attention.[16, 17] For the integration of MOF materials, however, the type of charge transport, such as hopping, band-like transport or incoherent tunneling, need to be analyzed in the context of existing charge transport models. As in the case of precisely determining MOF optical properties, MOF powders are not well suited for a thorough electrical characterization. The preparation of well-defined contacts to the electrodes makes the recording of reliable and reproducible data very challenging for the powder materials.

In particular, one type of MOFs, HKUST-1, has attracted considerable attention after Allendorf and coworkers demonstrated[16, 18] that the conductivity of SURMOFs made from this compound, which essentially behaves as a large band-gap insulator, can be increased by six orders of magnitude upon loading with an organic molecule, TCNQ (tetracyanoquinodimethane). By using a sophisticated mercury-drop method to measure the current as a function of applied voltage, Figure 3a, the thickness dependency of HKUST-1 SURMOF conductivity could be studied in a systematic fashion and the data allowed to demonstrate that the electric conductivity in the empty framework material can be described by an incoherent charge hopping,

resulting in an overall ohmic behavior.[19] In the same study, also the influence of ferrocene loading has been investigated in a quantitative fashion, Figure 3b. It could be demonstrated that the conductivity increased by about an order of magnitude upon loading with this molecule. Again, a charge transport mechanism involving an incoherent tunneling resulting in a roughly linear dependence of resistivity on thickness was found to be consistent with the data.
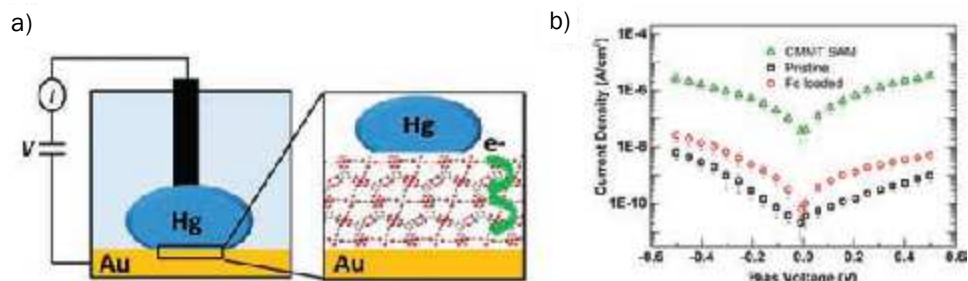
Fig. 3: a) Scheme of the mercury-droplet-based tunneling junction. Contact area between the two electrodes: Mercury-droplet as top electrode is passivated with a self-assembled monolayer (SAM) of hexadecanethiol ($C_{16}H_{33}$−SH), whereas the SURMOF grown on the CMMT-functionalized Au substrate serves as bottom electrode (CMMT: 9-carboxy-10-(mercaptomethyl) triptycene). b) Log current density J vs. voltage plot for HKUST-1 SUR-MOF, prepared by 5 spraying cycles, before (black empty squares) and after (red empty circles) the loading with ferrocene. Green empty triangles correspond to the CMMT SAM. Reproduced with permission form ref. [19]

In contrast to the electrical properties of ferrocene-loaded HKUST-1, the observed high conductivity of the same MOF loaded with TCNQ, however, was found to be difficult to reconcile with conventional transport mechanisms. A detailed investigation revealed that neither simple hopping nor band transport models are consistent with the experimental data determined with the mercury-drop method.[20] By using theoretical results to aid the interpretation of the experimental data, it could be demonstrated that the observed conductivity can be explained by an extended hopping transport model including virtual hops through localized MOF states. This mechanism is also referred to as molecular superexchange. Predictions on the basis of this model were found to show excellent agreement with the experimental data.[20]

UNIQUE MODEL SYSTEM FOR DIFFUSION EXPERIMENTS

For virtually all applications of nanoporous materials like zeolites, nanoporous carbons and MOFs, the loading with and diffusion of guest molecules within the voids govern the performance of these materials, e.g. as molecular containers or as membranes, in a crucial fashion. Therefore, the detailed understanding of the diffusion processes is pivotal, not just from a scientific point of view. Although there is a substantial progress in the understanding of diffusion and mass transfer of small molecules with relatively large diffusion coefficients in MOFs,[21, 22] the experimental determination of low diffusion coefficients, e.g. of large guest molecules, represents a challenging experimental task. Conventional techniques for investigating the diffusion in nanoporous materials, such as pulsed-field gradient nuclear magnetic resonance[23] and quasi-elastic neutron scattering[23], are usually not suitable for determining diffusion coefficients smaller than $10^{-12} m^2 s^{-1}$. The use of optical techniques like interference or infrared microscopy[22] for determining small diffusion coefficients is hindered by the fact that, for high-quality measurements, these methods require relatively large crystals of the nanoporous material (>50 μm). This results in very long uptake and release times for slow diffusion processes. As example, the uptake of molecules with a diffusion coefficient of $10^{18} m^2 s^{-1}$ by a MOF crystal with a size of 50 μm would last more than a year. On the other hand, the uptake by a 100 nm-thick film would take only 1 h.[24, 25]

Using a number of selected works, we will demonstrate here that SURMOFs are ideally suited as model systems to study diffusion in these porous, molecular frameworks (see Figure 4).
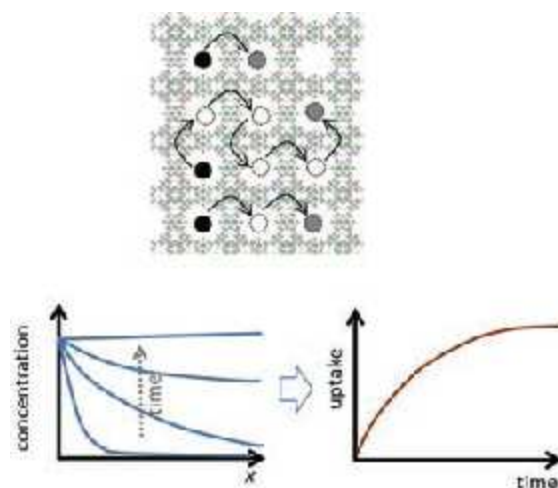
Fig. 4: Sketch of the molecular diffusion in MOFs. By random jumps, the molecules diffuse through the crystalline pore system. The movement is sketch by hopping form the black to the grey positions (top). For single-component mass transfer, the transport diffusion of the guest molecules results in a balance of the concentration gradients until a homogenous concentration is obtained (bottom left). The uptake by the MOF (bottom right), i.e. the concentration of the guest molecules integrated over the entire sample, can be measured by the mass changes of the sample, for instance by a quartz crystal microbalance.

The uptake of host molecules into a SURMOF form either the gas phase or the liquid phase can be studied conveniently by a quartz-crystal microbalance (QCM). By growing the SURMOFs directly on the top Au-electrode of the QCM sensors, the change in mass of the MOF thin films can be monitored in a straightforward fashion and allows for a quantitative determination of the number of guest molecules incorporated into the pores of the MOF. In addition to determining the total change in mass, the time-dependence of the QCM signal can be used to investigate the mass transfer.[25]

The first study[26, 27] based on this approach focused on loading SURMOFs of type HKUST-1 with pyridine from the gas phase. The total uptake amounted to about 11 molecules per HKUST-1 unit cell. Fitting the time-dependent QCM results using a theoretical expression based on a Fickian diffusion model revealed an efficient diffusion coefficient of pyridine in HKUST-1 of $D(300 K) = 2.4 \times 10^{-18} m^2 s^{-1}$. In addition to pure intracrystalline diffusion, the efficient diffusion coefficient may comprise contributions from other transport resistances, like surface barriers. Assuming thermally activated diffusion

and neglecting the influence of additional transport barriers, these data correspond to an activation energy for diffusion of 0.71 eV. This value is in good agreement with the results of *ab-initio* quantum chemistry calculations of pyridine bound the Cu^{++}-ions in the MOF lattice, $E_B = 0.69$ eV.

Another way to determine the activation energy for diffusion in MOF films was demonstrated by performing uptake experiments at different temperatures and using an Arrhenius plot. The activation energy for ferrocene diffusion in SURMOF films of type $Cu_2(ndc)_2(dabco)$ was found to amount to approximately +90 kJ mol^{-1} (0.93 eV).[28] A particular advantage of SURMOF samples is that they are rigidly attached to a solid support. This fact allows for investigating the uptake from the liquid- and from the gas-phase by the same sample.[29]

After having demonstrated the suitability for studying diffusion in MOFs by using SURMOFs, in particular in connection with the QCM, we will now discuss the so-called surface barrier phenomenon, which describes additional mass transfer barriers for the guest molecules in porous materials during the loading and release. It was shown in various experiments using large crystals of MOFs[30] and zeolites[31], that these materials possess an additional mass transfer resistance at the external crystal surface, hindering the guest molecules in entering and leaving the pore space. This apparently omnipresent mass transport barriers, usually referred to as surface barriers, show pronounced variations between different measurements, even when carried out for the same powder material synthesized in subsequent batches. As a result of these experimental difficulties, the diffusion of molecules in MOFs is often poorly understood on a quantitative level and, for different samples of the identical material, diffusion coefficients are frequently reported which differ by several orders of magnitude. For example, the experimental values reported for the diffusion coefficient of hydrogen in MOF-5 vary by four orders of magnitude, between 10^5 m^{2}s^1 (ref. [32]) and 10^9 m^{2}s^1 (ref. [33]). Even by comparing to results reported by the same group using the same synthesis procedure for the MOF material, variations by

many orders of magnitude can be found (diffusion coefficients of 10^9 m^{2}s^1 and 10^{12} m^{2}s^1, ref. [33, 34]).

In order to systematically study the surface barriers phenomenon in detail, thin, well-defined SURMOF films with an HKUST-1 structure were used.[34] By using a QCM, the uptake of a probe molecule, cyclohexane, by HKUST-1 SURMOFs of different thicknesses was investigated. In these experiments, we took advantage of the fact that the SURMOFs can be synthesized directly in the QCM cell without exposing the sample to the environment, like (humid) air. The sample mass and, thus, the SURMOF thicknesses were determined by QCM *in situ* during the synthesis. It was found that the uptake time of cyclohexane increases quadratically with the film thickness, Figure 5a.[34] Such a behavior is predicted by Fick's laws for pure diffusion-controlled uptake processes of a thin film (see Figure 5c left). Note, that the presence of a surface barrier (see Figure 5c right) results in a linear dependence of uptake time vs. film thickness. The observation of a quadratic increase thus immediately tells that the influence of surface barriers on the mass uptake of these pristine SURMOFs was negligible.[24] This is a clear demonstration that pristine, largely defect-free MOF materials do not possess surface barriers.

On the other hand, the mass transfer was found to tremendously slow down when exposing pristine HKUST-1 SURMOFs to humid air or water vapor, see figure 5b. In addition to the pronounced slowing down of the uptake kinetics as a result of this apparent corrosion, the time dependence as a function of film thickness would change from quadratic to linear. XRD data (see ref. [34]) showed that the bulk structure was unaffected by the exposure to water vapor or humid air; thus, it can be concluded that the hindrance of the uptake process is caused by structural inhomogeneities at the surface. It was proposed that the surface barriers were created by damaging the MOF structure at the surface, as a result of the water exposure. Since a short exposure to (humid) air or water vapor is already enough to cause the surface defects, this hypothesis well accounts for the fact that these surface barriers are so omnipresent.
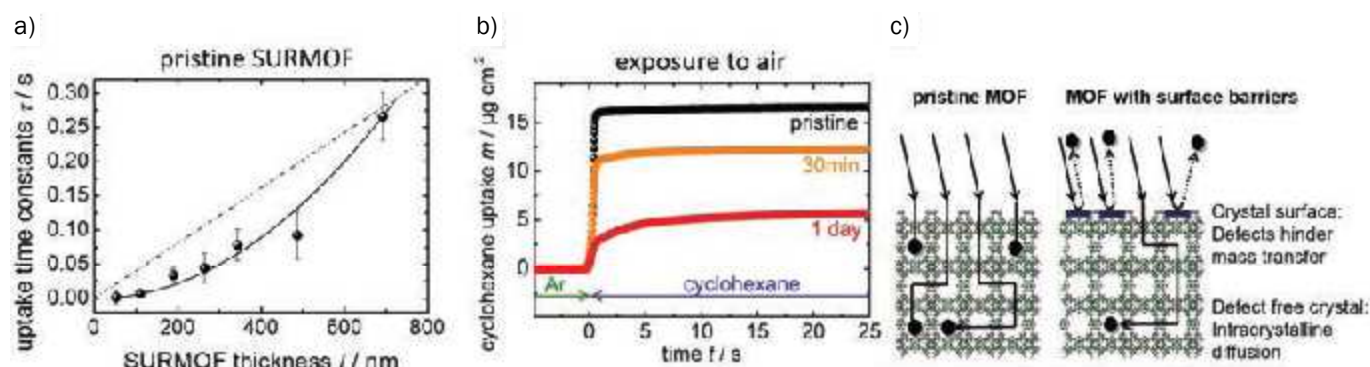
Fig. 5: **Surface barriers. a)** The time constants of the cyclohexane uptake by SURMOFs of various thicknesses are shown. The quadratic increase of time constant is a clear indication for the diffusion-limitation (solid line), rather than an influence of surface barriers. For surface-barrier-limited uptakes, uptake time and film thickness would be directly proportional (dotted line). **b)** Generating surface barriers. By exposing pristine SURMOFs to air for 30 min as well as for one day, the uptake amount is decreased and the uptake rate is tremendously slowed down. Since the samples were carefully activated before each uptake experiment, i.e. the pores were emptied at elevated temperature in pure argon flow, water molecules adsorbed in the pores can be excluded. **c)** Model of the mass transfer in MOFs. Left: unhindered mass transfer in the defect-free, nanoporous crystal, resulting in diffusion-limited uptake (solid line in a) Right: Surface barriers, caused by a large amount of completely blocked pores with only a few accessible entrances, hinder the guest molecules from entering the pore space and significantly slow down the mass transfer. Reproduced with permission form ref. [34]

STUDIES ON ENANTIOMER SEPARATION AND ANISOTROPY-EFFECTS IN CIRCULAR DICHROISM (CD)

Since MOFs can be fabricated using chiral linkers, they also establish an ideal model system for investigating enantiomer separation using chiral porous materials. As has been demonstrated above, SURMOFs allow for the monitoring of adsorption of guest molecules in MOF materials and the determination of the corresponding diffusion constants.[8, 26, 28] By employing chiral MOFs, the dependence of the uptake on the chirality of the guest molecules can be determined using QCM in a straightforward fashion. This is in contrast to the corresponding powder materials, where such uptake studies often require more complicated experimental procedures. Using the QCM-based approach, Liu et al.[35] have investigated pillared-layer SURMOFs of the type $Zn_2((+)cam)_2(dabco)$ ((+)cam=(1R,3S)-(+)-camphoric acid, dabco=1,4-diazabicyclo(2.2.2)octane)). After growing this enantiopure SURMOF directly on a QCM sensor, the authors could monitor the enantiopure uptake of a pair of chiral guest molecules, namely (2R,5R)-2,5-hexanediol and (2S,5S)-2,5-hexanediol. Here, the loading occurred from the gas phase under flow conditions. A pronounced difference in the uptake kinetics of the two different enantiomers was observed, with the time constant differing by about a factor of two. The total loading was different, also by a factor of two. Because QCM cannot distinguish the uptake of the two different enantiomers solely by the mass uptake, data on racemate separation cannot be gained using this approach. This limitation can be overcome by using circular dichroism (CD) to investigate the loading of chiral SURMOFs.

Indeed, Gu et al.[36] demonstrated that chiral SURMOFs based on camphoric acid with composition $Cu_2(Dcam)_{2x}(Lcam)_{2-2x}(dabco)$ are well suited to quantitatively investigate enantiomer separation and to demonstrate orientation effects in circular dichroism (CD) in the UV-vis range. In this case, three-dimensional chiral SURMOFs with a high degree of orientation were grown on quartz glass plates using the lbl method. The SURMOF growth orientation, as checked by XRD, could be varied between [001] and [110] by changing between OH- or COOH-terminated substrates. The CD data recorded for this chiral SURMOFs clearly demonstrated the presence of different CD signals for the differently oriented SURMOFs. Comparison to the results of theoretical work revealed good agreement and showed that the oriented CD band intensities of the enantiopure $Cu_2(Dcam)_2(dabco)$ grown in different orientations are a direct consequence of the anisotropic nature of the chiral SURMOFs. In a second set of experiments, the enantiopure $Cu_2(Dcam)_2(dabco)$ and $Cu_2(Lcam)_2(dabco)$ SURMOFs were loaded with the two chiral forms of ethyl-lactate, (+)-ethyl-D-lactate and (-)-ethyl-L-lactate. These results demonstrated an enantioselective enrichment of >60 % when loading the porous, chiral framework from the racemic mixture. Chiral SURMOFs thus constitute ideal model systems for studying enantiomer separation. A recent example is the study by Gu et al.[37], who investigated the effect of pore size on enantiomer selectivity. Their QCM uptake experiments with enantiopure R- and S-limonene clearly showed a pronounced influence of the MOF pore size on enantioselective adsorption in homochiral framework materials, although the chiral centers in the porous material were identical.

PHOTOSWITCHABLE NANOPOROUS COATING

The integration of stimuli-responsive molecules, i.e. molecules which respond to external signals such as light, heat, electric fields or pH-changes, into solids is an attractive way to render functionality to a material. A fairly large number of such chemical species are available, and the switching of numerous molecular functions was demonstrated.[38, 39] Since light is a simple and mostly nondestructive signal, photoswitchable molecules attract particular attention. In this context, an especially interesting and intensively investigated molecule is azobenzene. This compound has been used as smart moiety for various intriguing demonstrations of molecular functionality, including molecular machines like "nano-pliers"[40] or "nano-cars"[41]. The integration of such optical switches into solid materials remains, however, a major challenge. If the packing of azobenzene is too tight, e.g. in the bulk form of azobenzene, sterical constraints prohibit light-induced switching between the different azobenzene conformers. Nevertheless, intense, mostly trial-and-error based, research in this direction has allowed to identify a number of successful cases, such as the incorporation of azobenzene in polymers and cross-linked liquid crystal polymers (CLCPs). In these cases, macroscopic, light-induced responses resulting in changes in length and shape[42] of samples made from this optically active materials could be demonstrated. Based on the contraction and extension of the polymer, interesting applications like a photon-driven motor have been realized.[43] However, a precise prediction and a direct transfer of the variation of the molecular properties, like molecular length changes as well as dipole moment changes, to macroscopic variations of the materials are so far lacking. In addition, a thorough quantitative analysis allowing for a meaningful comparison with results from theoretical studies in such amorphous materials has not yet been possible. A different approach to realize smart light-responsive materials is based on self-assembled monolayers. In several cases the switching of macroscopic properties, e.g. its wettability,[44, 45] has been demonstrated. However, also in these cases, the influence of defects has been demonstrated to be huge.[46]

For quantitative studies, using structurally well-defined, crystalline systems containing sufficient free space, such as MOFs and in particular SURMOFs, offers a number of advantages. Azobenzene can be incorporated as dangling side groups in the nanoporous, crystalline MOF structure, see Figure 6a. The linkers used to fabricate the MOF can be chosen such that the transition from the *trans* to the *cis* conformation is not sterically hindered. Therefore, the photoisomerization of the azobenzene moiety and the resulting variations in the physical and chemical material properties of these optically active materials can be studied in a straightforward fashion. One of the most interesting applications of photoswitchable SURMOFs is the remote-controlled release of guest molecules, with e.g. biological or medical functionality. For this purpose, a hetero-bilayer SURMOF was fabricated, comprising a (passive) bottom layer, $Cu_2(BPDC)_2(BiPy)$,[47] acting as a container to store molecules, and on top a photoswitchable layer, $Cu_2(AzoBPDC)_2(BiPy)$. The top SURMOF has the same lattice parameters as the bottom layer and was designed to act as a valve, i.e. to open and close access to the container upon

irradiation with light. (BiPy: 4,4'-bipyridine, BPDC: biphenyl-4,4'-dicarboxylic acid, AzoBPDC: 2-azobenzene 4,4'-biphenyl-dicarboxylic acid). The reversible photoswitching of the azobenzene side group was investigated by UV-vis spectroscopy, where intensity changes of the $\pi \rightarrow \pi^*$ and $n \rightarrow \pi^*$ bands upon irradiation with UV or visible light can be observed. By QCM uptake experiments and using 1,4-butanediol as a probe molecule, the effect of the azobenzene photoswitching in the top layer on the mass transfer into and out of the SURMOF was investigated. The *trans*-to-*cis* photoswitching results in a reversible, significant decrease of the uptake rate constant (by a factor of 15), i.e. the permeability of the azobenzene-containing layer significantly decreases upon *trans*-to-*cis* isomerization. The opening and closing of the top layer enables the remote-controlled release from the nanoporous container. After loading the two-part SURMOF with the guest molecule, the top layer was switched to the *cis* state, i.e. closed. Then, the gas atmosphere above the sample was changed to pure argon. Although the desorption and release of the guest molecules was actually started, only a small release rate was observed by QCM, see Figure 6b. By irradiation of the sample with visible light, the top layer was switched to its *trans* state; thus, the top layer was opened and the release from the molecular container was initiated, as measured by QCM.

By using alkanes, alcohols and diols as probe molecules, it was shown that the switching effect, i.e. the difference in the loading by *trans* and *cis* SURMOF, is caused by the switching of the azobenzene dipole moment, which is 0 Debye in *trans* and 3 Debye in *cis,* and the dipole-dipole interaction (also referred to as Keesom interaction) with the guest molecules.[48]

The separation of molecular mixtures by nanoporous membranes is an ecologic alternative to energy-intensive distillation and cryogenic separation processes. Due to their large variety and the option of appropriate functionalizations adjusting the pore size, MOFs are a very promising material for efficient membrane separation. Recently, a demonstration of the unique properties of these porous framework materials has been provided by Wang *et al.,* who used membranes made from photoswitchable MOFs with azobenzene side groups. The authors could show that the selectivities of these membranes could be continuously varied over a wide range by illumination with light, Figure 7a. The SURMOFs used in this approach had a pillared-layer structure of type $Cu_2(AzoBPDC)_2(AzoBiPyB)$ (AzoBiPyB: 4,4'-(2-(phenyldiazenyl)-1,4-phenylene)dipyridine (or dipyridylazobenzene)[49]). The light-induced isomerization of the azobenzene side groups was studied by UV-vis and infrared spectroscopy. The *cis* azobenzene ratio was adjusted between 0 and 63 % by irradiating the sample with UV light (*trans*-to-*cis*) or blue light (*cis*-to-*trans*) for short illumination times or by simultaneous irradiation with blue and UV light. The SURMOFs were deposited on mesoporous supports and the separation of binary H_2:CO_2 mixture was investigated. By using a Wicke-Kallenbach setup where the membrane can be irradiated *in situ*, the photoswitchable membrane separation was measured.[50] The selection factor can be reversibly switched between 3 and 8 by UV and blue light irradiation, i.e. by *trans*-*cis* switching the azobenzene side groups, see Figure 7b. In addition, adjusting the *cis* azobenzene ratio between the minimum (0%) and the maximum (63%) value enables the fine-tuning of the separation factor, see Figure 7c. So, the molecular composition of the permeate flux can be continuously adjusted in a dynamic, remote-controlled fashion.
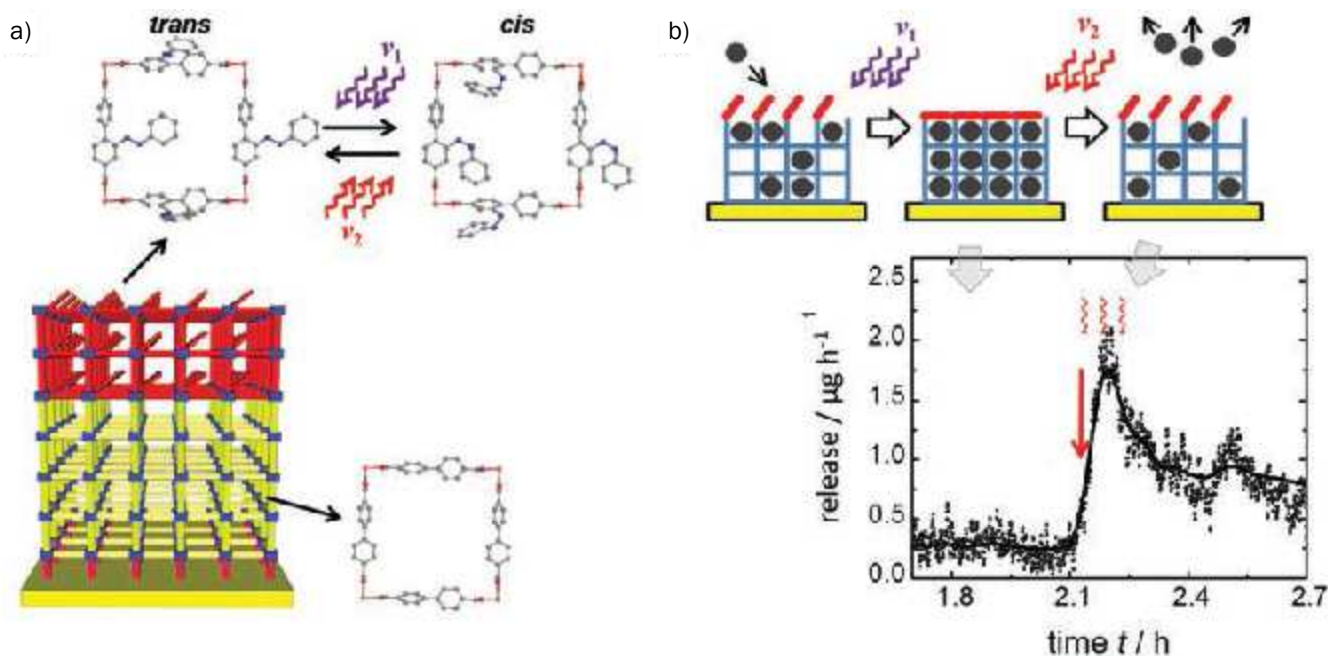
Fig. 6: Two-part photoswitchable SURMOF for remote-controlled release of guest molecules. a) The bottom $Cu_2(BPDC)_2(BiPy)$ layer (yellow) acts as a container to store molecules with the photoswitchable $Cu_2(AzoBPDC)_2(BiPy)$ layer (red) on top. The pore windows in the [001] direction are shown. The azobenzene side groups in the top layer can be reversibly switched from *trans*-to-*cis* by UV light and from *cis*-to-*trans* by visible light. While the azobenzene moiety is planar and nonpolar in the *trans* state, the moiety is bent and has a dipole moment of about 3 D in the *cis* state. b) Demonstration of optically triggered release from a molecular container. The two-part SURMOF was loaded with guest molecules, butanediol, and the top layer was closed by irradiation with UV light ν₁. Although the release was started, only a minor leakage rate was measured by QCM until the top layer was switched to *trans*, i.e. opened, by irradiation with visible light ν₂. Reprint with permission from ref. [47].
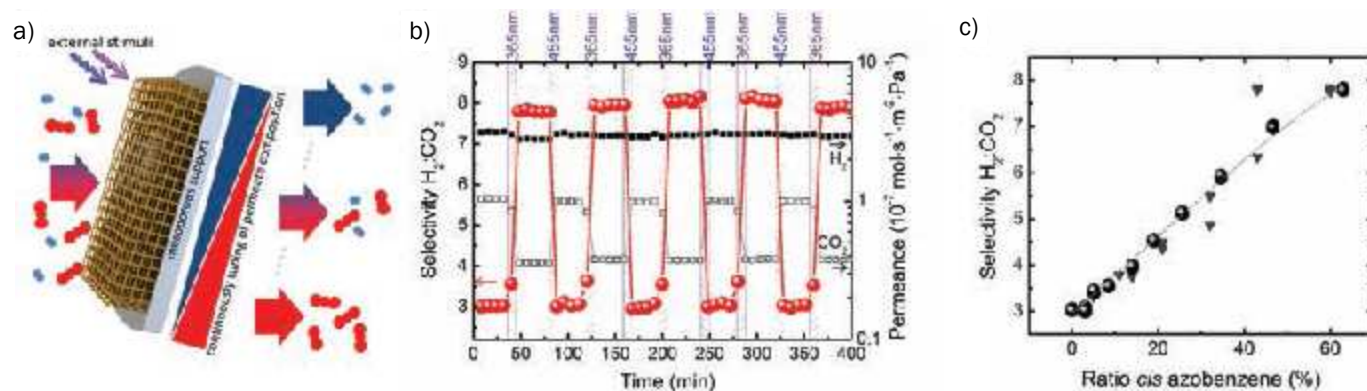
Fig. 7: Tunable molecular separation by photoswitchable MOF membranes. a) Illustration of remote-controllable, continuously tunable molecular selectivity by a photoswitchable MOF membrane, separating the molecular feed mixture (blue and red molecules). b) Separation of H_2:CO_2 mixture where the membrane was irradiated with 365 nm (*cis*) and 455 nm (*trans*) for 5 min each. Permeances of CO_2 and H_2 are shown as black open squares and solid squares; the molecular selectivities (or separation factors) are shown as red spheres. c) H_2:CO_2 separation factor versus the ratio of *cis* azobenzene. Adjusting the *cis*-azobenzene ratio, which can be realized by brief illumination times or by simultaneous irradiation with blue and UV light, results in a continuous tuning of the selectivity. Reprint with permission from ref. [50].

AZOBENZENE-CONTAINING SURMOFS AS MODEL SYSTEM FOR MOLECULAR PHOTOSWITCHES

In addition to functional coatings, azobenzene-containing SUR-MOF serves as model system for precise measurements of molecular properties. Bulk (plain) azobenzene is a crystalline solid at room temperature and shows no photoswitching behavior.[51] On the other hand, photoswitching of azobenzene can be directly observed in the gas phase[5], in solution or incorporated in a polymer, where the specific dynamics (i.e. energy barriers, switching rate, relaxation times, etc.) depend on the molecular environment.[52-54] For instance, the thermal *cis*-to-*trans* isomerization and the stability of *cis* azobenzene adsorbed on various surfaces,[55] adsorbed in small pores,[56] in solution,[57] or incorporated in polymers[58] varies significantly.

Azobenzene-containing SURMOFs with large pore sizes, where the azobenzene side groups point into the pores and have no interaction with other parts of the framework, serve as unique model system to investigate the isomerization of isolated azobenzene moieties, see Figure 8a.[59] The isomerization was investigated in ultrahigh vacuum (UHV) at different temperatures by infrared reflection absorption spectroscopy (IRRAS), see Figure 8b. After UV irradiation, the rate constants of the decay of *cis* azobenzene and of the increase of *trans* azobenzene in the

dark were used for an Arrhenius plot, see Figure 8c, and an activation energy for the *cis*-to-*trans* isomerization of 1.09 eV ± 0.09 eV was determined. This value is in very good agreement with the activation energy for pure azobenzene determined by theoretical calculations.[60]

TRANSFER OF ELECTRONIC EXCITATIONS ACROSS ORGANIC/ORGANIC-HETEROJUNCTIONS

SURMOFs also offer a very interesting possibility to create model systems for studying the transfer of optical or electronic excitations across organic-organic interfaces. By choosing two different MOF types, A and B, with similar crystal structure and linkers of the same lengths but different properties, epitaxial growth of B on A can be realized, yielding a well-defined hetero-interface. If the organic linkers are based on chormophores, the transfer of optical excitation from one type of chromophore to a different type of chromophore can be studied. The fabrication of such well-defined interfaces is difficult to achieve e.g. for the normal, bulk form of such chromophores, which typically adopt rather different crystal structures.

In a first application of this approach, the Dexter energy transfer of triplet excitons over organic/organic heterojunctions has
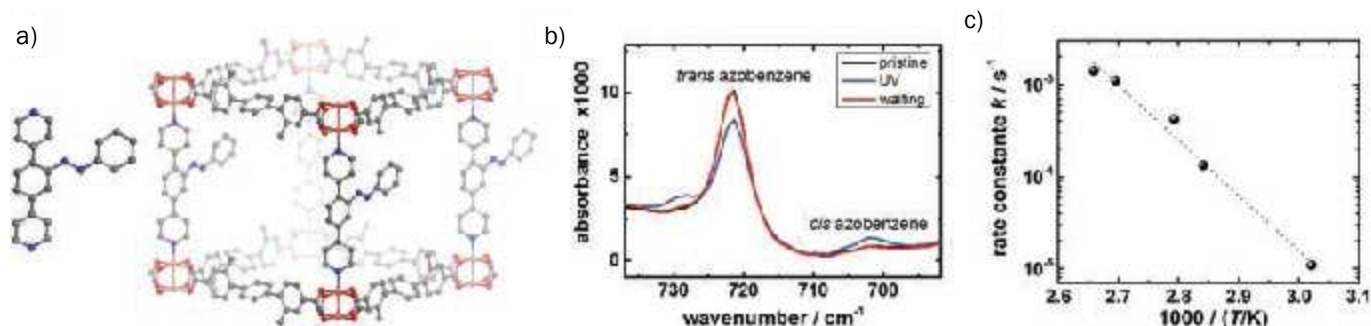
Fig. 8: Thermal relaxation of azobenzene in large-pore SURMOFs. a) AzoBiPyB linkers are included in the structure of Cu_2(DMTPDC)$_2$(AzoBiPyB) SURMOF, resulting in virtually isolated azobenzene side groups. The Cu atoms are plotted orange, O red, C grey, N blue and H is not shown. b) IRRA spectra of the Cu_2(DMTPDC)$_2$(AzoBiPyB) SURMOF before (black, *trans*), after UV irradiation (blue, *trans* and *cis*) and after the thermal relaxation to the *trans* state (red). The red and black spectra are practically identical. c) Arrhenius plot of the *cis*-to-*trans* rate constants determined from the changes of the IR bands. The activation energy is determined from the slope, dotted line. Reprint with permission from ref. [59].
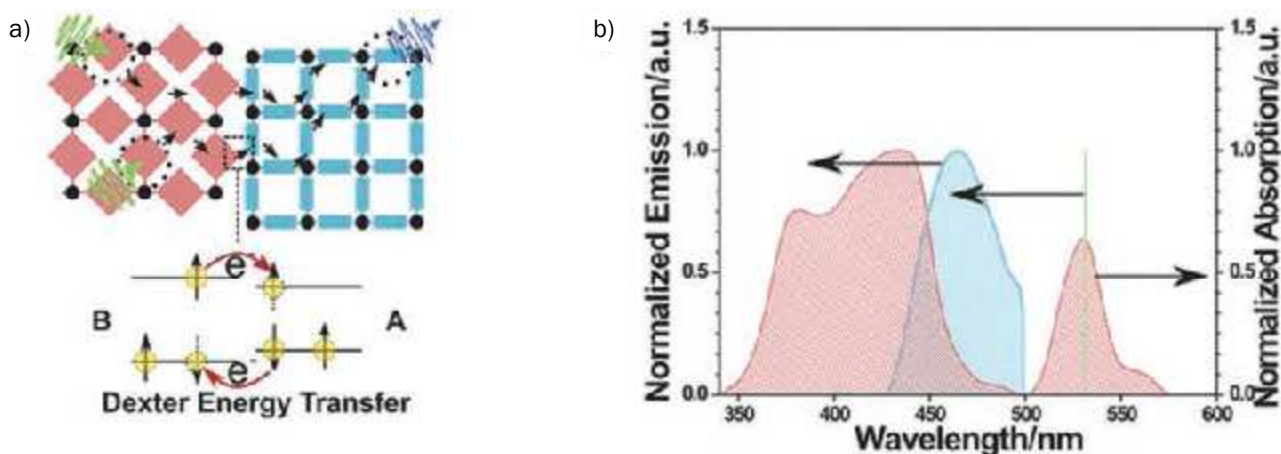
Fig. 9: a) Schematic diagram of triplet–triplet annihilation upconversion (TTA-UC) wherein two 532 nm photons absorbed by the sensitizer (B) SURMOF create triplet states that upon reaching the interface can transfer to the emitter (A) SURMOF by a Dexter two-electron-exchange mechanism. When two triplets meet in the emitter layer they can annihilate and emit a single higher-energy photon. b) The absorption spectrum of sensitizer (B) layer is shown in red and the wavelength of the 532 nm excitation laser is shown in green. The observed upconverted emission is shown in blue. The observation of upconverted emission provides direct optical evidence that the SURMOF−SURMOF heterojunction is of sufficient quality to allow triplet, and therefore necessarily also electron, transfer between the SURMOF layers. Reprint with permission from ref. 6.

been studied using the SURMOF approach. Two different, chromophore-based linkers were used, Pd-DCP (Pd(II)5,15-diphenyl-10,20-di(4-carboxyphenyl) porphyrin) and ADB (4,4'-(anthracene-9,10-diyl)dibenzoate).[6] It was demonstrated that these hetero-junctions show solid-state photon up-conversion (UC), green photons were converted to blue, Figure 9. An intentional variation of the structural property of the interfaces between the ADB and Pd-DCP SURMOFs in this work demonstrated that the quality of the interface has substantial influence on the up-conversion properties. Since these heterojunctions are structurally well-defined, they offer an excellent basis for comparison to the results of theoretical works.

SUMMARY

In this overview we have demonstrated several cases where highly oriented, crystalline, thin films of metal-organic frameworks, MOFs, have been used as model systems to study molecular interactions in porous solids. In addition to phenomena related to diffusion, such as diffusion constants, activation energies and the importance of defects, also other physical properties, e.g. electrical conduction mechanisms and optical properties, can be studied. Particularly interesting is the possibility to investigate and utilize light-induced switching of molecules, a topic with relevance to the construction of molecular machines.

REFERENCES

[1]   S. Kaskel, The Chemistry of Metal-Organic Frameworks: Synthesis, Characterization, and Applications. (Wiley, 2016).

[2]   P. Z. Moghadam, A. Li, S. B. Wiggin, A. Tao, A. G. P. Maloney, P. A. Wood, S. C. Ward and D. Fairen-Jimenez, *Chem. Mat.* **29** (7), 2618-2625 (2017).

[3]   H. X. Deng, S. Grunder, K. E. Cordova, C. Valente, H. Furukawa, M. Hmadeh, F. Gandara, A. C. Whalley, Z. Liu, S. Asahina, H. Kazumori, M. O'Keeffe, O. Terasaki, J. F. Stoddart and O. M. Yaghi, *Science* **336** (6084), 1018-1023 (2012).

[4]   C. E. Wilmer, M. Leaf, C. Y. Lee, O. K. Farha, B. G. Hauser, J. T. Hupp and R. Q. Snurr, *Nature Chemistry* **4** (2), 83-89 (2012).

[5]   L. Duarte, R. Fausto and I. Reva, *Physical Chemistry Chemical Physics* **16** (32), 16919-16930 (2014).

[6]   M. Oldenburg, A. Turshatov, D. Busko, S. Wollgarten, M. Adams, N. Baroni, A. Welle, E. Redel, C. Woll, B. S. Richards and I. A. Howard, *Adv. Mater.* **28** (38), 8477-8482 (2016).

[7]   J. Liu and C. Wöll, *Chem. Soc. Rev.* DOI: 10.1039/c7cs00315c (2017).

[8]   L. Heinke, M. Tu, S. Wannapaiboon, R. A. Fischer and C. Wöll, *Microporous Mesoporous Mat.* **216**, 200-215 (2015).

[9]   Z. Wang, P. G. Weidler, C. Azucena, L. Heinke and C. Wöll, *Microporous Mesoporous Mat.* **222**, 241-246 (2016).

[10] M. Tafipolsky, S. Amirjalayer and R. Schmid, *J. Phys. Chem. C* **114** (34), 14402-14409 (2010).

[11] P. St Petkov, G. N. Vayssilov, J. X. Liu, O. Shekhah, Y. M. Wang, C. Wöll and T. Heine, *ChemPhysChem* **13** (8), 2025-2029 (2012).

[12] Z. B. Wang, H. Sezen, J. X. Liu, C. W. Yang, S. E. Roggenbuck, K. Peikert, M. Froba, A. Mavrantonakis, B. Supronowicz, T. Heine, H. Gliemann and C. Woll, *Microporous Mesoporous Mat.* **207**, 53-60 (2015).

[13] Z.-G. Gu, A. Pfriem, S. Hamsch, H. Breitwieser, J. Wohlgemuth, L. Heinke, H. Gliemann and C. Wöll, *Microporous Mesoporous Mat.* **211**, 82-87 (2015).

[14] Z. Gu, L. Heinke, C. Wöll, T. Neumann, W. Wenzel, Q. Li, K. Fink, O. D. Gordan and D. R. T. Zahn, *Applied Physics Letters* **107**, 183301 (2015).

[15] H. Furukawa, K. E. Cordova, M. O'Keeffe and O. M. Yaghi, *Science* **341** (6149), 1230444 (2013).

[16] V. Stavila, A. A. Talin and M. D. Allendorf, *Chemical Society Reviews* **43** (16), 5994-6010 (2014).

[17] P. Falcaro, R. Ricco, C. M. Doherty, K. Liang, A. J. Hill and M. J. Styles, *Chemical Society Reviews* **43** (16), 5513-5560 (2014).

[18] A. A. Talin, A. Centrone, A. C. Ford, M. E. Foster, V. Stavila, P. Haney, R. A. Kinney, V. Szalai, F. El Gabaly, H. P. Yoon, F. Leonard and M. D. Allendorf, *Science* **343** (6166), 66-69 (2014).

[19] J. Liu, T. Wächter, A. Irmler, P. G. Weidler, H. Gliemann, F. Pauly, V. Mugnaini, M. Zharnikov and C. Wöll, *ACS Applied Materials & Interfaces* **7** (18), 9824-9830 (2015).

[20] T. Neumann, J. Liu, T. Waechter, P. Friederich, F. Symalla, A. Welle, V. Mugnaini, V. Meded, M. Zharnikov, C. Woell and W. Wenzel, *ACS Nano* **10** (7), 7085-7093 (2016).

[21] T. Titze, A. Lauerer, L. Heinke, C. Chmelik, N. E. R. Zimmermann, F. J. Keil, D. M. Ruthven and J. Karger, *Angew. Chem.-Int. Edit.* **54** (48), 14580-14583 (2015).

[22] J. Kärger, T. Binder, C. Chmelik, F. Hibbe, H. Krautscheid, R. Krishna and J. Weitkamp, *Nat Mater* **13** (4), 333-343 (2014).

[23] H. Paoli, A. Methivier, H. Jobic, C. Krause, H. Pfeifer, F. Stallmach and J. Kärger, *Microporous Mesoporous Mat.* **55** (2), 147-158 (2002).

[24] J. Kärger, D. M. Ruthven and D. N. Theodorou, Diffusion in Nanoporous Materials. (Wiley-VCH, 2012).

[25] L. Heinke, *Journal of Physics D: Applied Physics* **50**, 193004 (2017).

[26] O. Zybaylo, O. Shekhah, H. Wang, M. Tafipolsky, R. Schmid, D. Johannsmann and C. Wöll, *Physical Chemistry Chemical Physics* **12** (28), 8092-8097 (2010).

[27] O. Zybaylo, O. Shekhah, H. Wang, M. Tafipolsky, R. Schmid, D. Johannsmann and C. Woll, *Physical Chemistry Chemical Physics* **15** (48), 21099-21099 (2013).

[28] L. Heinke and C. Wöll, *Physical Chemistry Chemical Physics* **15** (23), 9295-9299 (2013).

[29] W. Zhou, C. Wöll and L. Heinke, *Materials* **8** (6), 3767 (2015).

[30] F. Hibbe, C. Chmelik, L. Heinke, S. Pramanik, J. Li, D. M. Ruthven, D. Tzoulaki and J. Kärger, *J. Am. Chem. Soc.* **133** (9), 2804-2807 (2011).

[31] J. C. Saint Remi, A. Lauerer, C. Chmelik, I. Vandendael, H. Terryn, G. V. Baron, J. F. M. Denayer and J. Kärger, *Nat. Mater.* **15** (4), 401-+ (2016).

[32] C. Xu, J. Yang, M. Veenstra, A. Sudik, J. J. Purewal, Y. Ming, B. J. Hardy, J. Warner, S. Maurer, U. Müeller and D. J. Siegel, *International Journal of Hydrogen Energy* **38** (8), 3268-3274 (2013).

[33] D. Saha, Z. Wei and S. Deng, *Separation and Purification Technology* **64** (3), 280-287 (2009).

[34] L. Heinke, Z. Gu and C. Wöll, *Nat Commun* **5**, 4562 (2014).

[35] B. Liu, O. Shekhah, H. K. Arslan, J. Liu, C. Wöll and R. A. Fischer, *Angewandte Chemie International Edition* **51** (3), 807-810 (2012).

[36] Z.-G. Gu, J. Bürck, A. Bihlmeier, J. Liu, O. Shekhah, P. G. Weidler, C. Azucena, Z. Wang, S. Heissler, H. Gliemann, W. Klopper, A. S. Ulrich and C. Wöll, *Chemistry – A European Journal* **20** (32), 9879-9882 (2014).

[37] Z. Gu, S. Grosjean, S. Bräse, C. Wöll and L. Heinke, *Chemical Communications* **51**, 8998-9001 (2015).

[38] W. R. Browne and B. L. Feringa, *Nature Nanotechnology* **1** (1), 25-35 (2006).

[39] B. L. Feringa and W. R. Browne, Molecular Switches. (Wiley, 2011).

[40] T. Muraoka, K. Kinbara and T. Aida, *Nature* **440** (7083), 512-515 (2006).

[41] G. Vives and J. M. Tour, *Accounts of Chemical Research* **42** (3), 473-487 (2009).

[42] Z. Mahimwalla, K. G. Yager, J. Mamiya, A. Shishido, A. Priimagi and C. J. Barrett, *Polymer Bulletin* **69** (8), 967-1006 (2012).

[43] M. Yamada, M. Kondo, J.-i. Mamiya, Y. Yu, M. Kinoshita, C. J. Barrett and T. Ikeda, *Angew. Chem.-Int. Edit.* **47** (27), 4986-4988 (2008).

[44] A. M. Masillamani, S. Osella, A. Liscio, O. Fenwick, F. Reinders, M. Mayor, V. Palermo, J. Cornil and P. Samori, *Nanoscale* **6** (15), 8969-8977 (2014).

[45] W. Freyer, D. Brete, R. Schmidt, C. Gahl, R. Carley and M. Weinelt, *Journal of Photochemistry and Photobiology a-Chemistry* **204** (2-3), 102-109 (2009).

[46] T. Weidner, F. Bretthauer, N. Ballav, H. Motschmann, H. Orendi, C. Bruhn, U. Siemeling and M. Zharnikov, *Langmuir* **24** (20), 11691-11700 (2008).

[47] L. Heinke, M. Cakici, M. Dommaschk, S. Grosjean, R. Herges, S. Bräse and C. Wöll, *Acs Nano* **8** (2), 1463-1467 (2014).

[48] Z. Wang, S. Grosjean, S. Braese and L. Heinke, *ChemPhysChem* **16** (18), 3779-3783 (2015).

[49] Z. Wang, L. Heinke, J. Jelic, M. Cakici, M. Dommaschk, R. J. Maurer, H. Oberhofer, S. Grosjean, R. Herges, S. Bräse, K. Reuter and C. Wöll, *Phys. Chem. Chem. Phys.* **17**, 14582 – 14587 (2015).

[50] Z. Wang, A. Knebel, S. Grosjean, D. Wagner, S. Bräse, C. Wöll, J. Caro and L. Heinke, *Nature Communications* **7**, 13872 (2016).

[51] M. Tsuda and K. Kuratani, Bull. *Chem. Soc. Jpn.* **37** (9), 1284-1288 (1964).

[52] A. Natansohn and P. Rochon, *Chemical Reviews* **102** (11), 4139-4175 (2002).

[53] Y. Imai, K. Naka and Y. Chujo, *Macromolecules* **32** (4), 1013-1017 (1999).

[54] S. Deshmukh, L. Bromberg, K. A. Smith and T. A. Hatton, *Langmuir* **25** (6), 3459-3466 (2009).

[55] J. Henzl, M. Mehlhorn, H. Gawronski, K. H. Rieder and K. Morgenstern, *Angew. Chem.-Int. Edit.* **45** (4), 603-606 (2006).

[56] Y. Kuriyama and S. Oishi, *Chemistry Letters* (10), 1045-1046 (1999).

[57] J. Dokic, M. Gothe, J. Wirth, M. V. Peters, J. Schwarz, S. Hecht and P. Saalfrank, *Journal of Physical Chemistry A* **113** (24), 6763-6773 (2009).

[58] C. D. Eisenbach, *Makromolekulare Chemie-Macromolecular Chemistry and Physics* **179** (10), 2489-2506 (1978).

[59] X. Yu, Z. Wang, M. Buchholz, N. Fullgrabe, S. Grosjean, F. Bebensee, S. Bräse, C. Wöll and L. Heinke, *Physical Chemistry Chemical Physics* **17**, 22721 – 22725 (2015).

[60] A. Cembran, F. Bernardi, M. Garavelli, L. Gagliardi and G. Orlandi, *J. Am. Chem. Soc.* **126** (10), 3234-3243 (2004).